HAL open science

A Single Observer for Currents Estimation in Sensor's Fault-Tolerant Control of Induction Motor Drives

Younes Azzoug, Remus Pusca, Mohamed Sahraoui, Abdelkarim Ammar, Raphael Romary, Antonio J Marques Cardoso

To cite this version:

Younes Azzoug, Remus Pusca, Mohamed Sahraoui, Abdelkarim Ammar, Raphael Romary, et al.. A Single Observer for Currents Estimation in Sensor's Fault-Tolerant Control of Induction Motor Drives. 2019 International Conference on Applied Automation and Industrial Diagnostics (ICAAID), Sep 2019, Elazig, Turkey. pp.1-6, 10.1109/ICAAID.2019.8934969 . hal-03276632

HAL Id: hal-03276632

https://univ-artois.hal.science/hal-03276632v1

Submitted on 2 Jul 2021

HAL is a multi-disciplinary open access archive for the deposit and dissemination of scientific research documents, whether they are published or not. The documents may come from teaching and research institutions in France or abroad, or from public or private research centers.

L'archive ouverte pluridisciplinaire **HAL**, est destinée au dépôt et à la diffusion de documents scientifiques de niveau recherche, publiés ou non, émanant des établissements d'enseignement et de recherche français ou étrangers, des laboratoires publics ou privés.

A Single Observer for Currents Estimation in Sensor's Fault-Tolerant Control of Induction Motor Drives

Younes Azzoug
Department of Electrical Engineering of the University of Biskra
Laboratory of Electrical Engineering of Biskra (LGEB)
Biskra, Algeria
younes.azzoug@univ-biskra.dz

Remus Pusca
Faculty of Applied Science
Univ. Artois, EA 4025 LSEE F-62400
Bethune, France
remus.pusca@univ-artois.fr

Mohamed Sahraoui
Department of Electrical Engineering of the University of Biskra
Laboratory of Electrical Engineering of Biskra (LGEB)
Biskra, Algeria
m.sahraoui@univ-biskra.dz

Abdelkarim Ammar
Institute of Electrical and Electronics Engineering
Signal and Systems Laboratory
Boumerdes, Algeria
a.ammar@univ-boumerdes.dz

Raphael Romary
Faculty of Applied Science
Univ. Artois, EA 4025 LSEE F-62400
Bethune, France
raphael.romary@univ-artois.fr

Antonio J. Marques Cardoso
CISE - Electromechatronic Systems Research Centre
Universidade da Beira Interior
Covilhã, Portugal
ajmcardoso@ieee.org

***Abstract*— This paper proposes a fault-tolerant control technique against current sensors failure in direct torque controlled induction motors drives. Several important aspects are covered in the proposed algorithm, such as the detection of sensors failure, the isolation of faulty sensors, and the reconfiguration of the control system by a correct estimation. A logic circuit ensures fault detection by analyzing the residual signal between the measured and estimated quantities, while a single modified Luenberger observer performs the task of estimating the line currents, even when all the sensors are in the faulty state. In addition, a decision logic circuit isolates the erroneous signal and simultaneously selects the appropriate estimated current signal. The proposed scheme is tested on MATLAB/Simulink environment and experimentally validated in a laboratory prototype mainly containing a dS1104 card and 4 kW induction motor.**

Keywords—fault tolerant control, fault detection, current estimation, induction motor, direct torque control, adaptive observer.

I. INTRODUCTION

Fault Tolerant Control (FTC) methods are crucial in variable speed drives used in critical and high-sensitivity applications, such as, space exploration, nuclear power plants, electric vehicles, air and rail transportation; in order to ensure system security, and uninterrupted operation, even with degraded performance, when an unexpected failure occurs in the variable speed drive. Consequently, a fault tolerant control strategy must be implemented to guarantee that faults are handled in such a way that there will be no damage.

Generally, variable speed Induction Motor (IM) drives need feedback information from a speed/position transducer, two or three current sensors and a dc-link voltage sensor at least [1], [2]. Unfortunately, sensors are very prone to failures, and for this reason several research results have been published regarding sensors fault-tolerant control, as well as Fault Detection, Isolation, and Reconfiguration (FDIR) methods [3]–[10].

The study in [3] presents a sensor FTC of an induction motor drive, based on the extended Kalman filter, and a reduced number of adaptive observers, to keep the operation of the system under the occurrence of sensors failures. In [4], a fault-tolerant vector control is proposed. A logic circuit is used to identify the faulty current sensor. The missing current information is replaced by an appropriate stator current, which value is calculated from algebraic equations and from the other measured healthy currents. However, this approach is not practical in the event of a successive failure in the different sensors. A fault-tolerant control scheme is proposed in [5], in which an adaptive fuzzy logic-based observer is used to generate residuals, which analysis allows the detection, and isolation of the faulty sensor. However, the dynamic response of this scheme for isolating defective sensors is too slow. In [6], it is proposed a sensor fault detection and isolation scheme for an IM drive, based on currents estimation and rotor resistance variations, which are then used in a decision unit for the identification and isolation of the faulty sensor. In [7], a FTC technique against speed and current sensors failures in IM drives is proposed, and based on three adaptive observers with different inputs. However, this method is not suitable to achieve an efficient FTC in case of failures in two or three sensors. The results obtained in [8] offer a solution to the succession of faults in the different sensors but the number of the used adaptive observers is still three. Another type of FTC methods has been also presented in the literature, in which the sensors FTC algorithm changes the control according to the type of the faulty sensor, as proposed in [11]–[14]. A smooth FTC of IM drives with sensor failures is presented in [11], [12]. In the healthy state, the IM drive's operation is accomplished using direct torque control; indirect field oriented control is then used when the dc-link voltage sensor fails, and v/f control is utilized during current sensors failure. The major drawback of this method, as reported in [15], is that these techniques are experimentally difficult to implement.

This paper proposes a direct torque fault-tolerant control strategy for the current sensors failure in induction motor drives. Some features are distinct from the other proposed methods. First, the estimation of stator currents is performed using a single observer. Then, the method proposed here allows the detection of faulty sensors even when several sensors fail successively, case in which a decision unit, based on a logic circuit, performs the task of reconfiguring and isolating the effects corresponding to the faulty sensor. Finally, the proposed technique can be reorganized in an

adaptive way in the event of the loss of one or two sensors. The proposed scheme is simulated in MATLAB/Simulink environment, and experimentally implemented in a laboratory test bench under different operating conditions.

The remainder of the paper is organized into V sections. Section II analyses the direct torque control. Afterwards, section III describes the concept of the proposed FTC. Simulation and experimental results are presented and discussed in section IV. Finally, section V presents the main conclusion of the paper.

II. Direct Torque Control of the Induction Motor

The system equation below gives the induction motor model used in the present work.

$$\begin{cases} \frac{di_{s\alpha}}{dt} = -\left(\frac{R_s}{\sigma L_s} + \frac{R_r}{\sigma L_r}\right) i_{s\alpha} - \omega_r i_{s\beta} + \frac{R_s}{\sigma L_s L_r}\psi_{s\alpha} + \frac{\omega_r}{\sigma L_r}\psi_{s\beta} + \frac{1}{\sigma L_s} V_{s\alpha} \\ \frac{di_{s\beta}}{dt} = -\left(\frac{R_s}{\sigma L_s} + \frac{R_r}{\sigma L_r}\right) i_{s\beta} - \omega_r i_{s\alpha} + \frac{R_s}{\sigma L_s L_r}\psi_{s\beta} + \frac{\omega_r}{\sigma L_r}\psi_{s\alpha} + \frac{1}{\sigma L_s} V_{s\beta} \\ \frac{d\psi_{s\alpha}}{dt} = V_{s\alpha} - R_s i_{s\alpha} \\ \frac{d\psi_{s\beta}}{dt} = V_{s\beta} - R_s i_{s\beta} \end{cases} \quad (1)$$

where:

$V_{s\alpha}, V_{s\beta}$: (α, β) stator voltages,
$i_{s\alpha}, i_{s\beta}$: (α, β) stator currents,
$\psi_{s\alpha}, \psi_{s\beta}$: (α, β) stator fluxes,
R_s, R_r : stator and rotor resistances,
L_s, L_r : stator and rotor inductances,
ω_r : rotor angular speed.
$\sigma = 1 - \frac{M^2}{L_s L_r}$, given that M is the mutual inductance.

The electromagnetic torque is expressed by the following equation:

$$T_e = p(\psi_{s\alpha} i_{s\beta} + \psi_{s\beta} i_{s\alpha}) \quad (2)$$

The stator flux components are given in the system equation below:

$$\begin{cases} \psi_{s\alpha} = \int (V_{s\alpha} - R_s i_{s\alpha}) dt \\ \psi_{s\beta} = \int (V_{s\beta} - R_s i_{s\beta}) dt \end{cases} \quad (3)$$

The Direct Torque Control (DTC) basic idea is to estimate flux and torque instaneous values only from the stator variables. The estimated torque is compared with the reference one given by the speed controller (PI controller in the present work), the resulting torque error signal is sent to an hysterisis controller (three-levels hysterisis controller is adopted in the present work) to get a control signal C_{Te}, which fed a switching look-up table. Likewise to the estimated flux, which is compared with fixed value of a stator flux magnitude, the resulting flux error signal is fed an hysterisis controller (two-levels hysterisis controller is adopted in the present work) to get a control signal C_{flx} for the switchin look-up table. This latter uses flux and torque control signals in order to generate three control signals S_A, S_B and S_C for the three-phase inverter (see Fig. 4).

III. Concept of the Proposed Fault-Tolerant Control

In the proposed fault-tolerant direct torque control, two current sensors in phase-a, and phase-b are used in addition to a dc-link voltage sensor, and an incremental encoder. Furthermore, using the control signals S_A, S_B and S_C, a voltage synthesizer construct the three-phase stator voltages applied to the machine from the voltage measured in the dc-link.

A. Stator Currents Estimation

In order to estimate the line currents, a modified adaptive observer is used, which gives high-performance estimation stator currents, based on the IM model, which is described by the following state equation:

$$\begin{cases} \dot{X} = A(\omega_r)X + BU \\ Y = CX \end{cases} \quad (4)$$

where:

$X = [i_{s\alpha}\ i_{s\beta}\ \psi_{r\alpha}\ \psi_{r\beta}]^T; \quad Y = [i_{s\alpha}\ i_{s\beta}]^T;$

$U = [V_{s\alpha}\ V_{s\beta}]^T$

and:

$$A = \begin{bmatrix} a_1 & 0 & a_2 & \omega_r a_3 \\ 0 & a_1 & -\omega_r a_3 & a_2 \\ a_4 & 0 & a_5 & -\omega_r \\ 0 & a_4 & \omega_r & a_5 \end{bmatrix}; \quad B = \begin{bmatrix} \frac{1}{\sigma L_s} & 0 \\ 0 & \frac{1}{\sigma L_s} \\ 0 & 0 \\ 0 & 0 \end{bmatrix};$$

$$C = \begin{bmatrix} 1 & 0 & 0 & 0 \\ 0 & 1 & 0 & 0 \end{bmatrix}$$

as well as:

$$a_1 = -\left(\frac{1}{\tau_s \sigma} + \frac{(1-\sigma)}{\tau_r \sigma}\right); \quad a_2 = \frac{M}{\sigma L_s L_r \tau_r}; \quad a_3 = \frac{M}{\sigma L_s L_r};$$

$$a_4 = \frac{M}{\tau_r}; \quad a_5 = \frac{1}{\tau_r}; \quad \tau_s = \frac{L_s}{R_s}; \quad \tau_r = \frac{L_r}{R_r};$$

The idea of the proposed stator currents estimator is based on the general theory of Luenberger observer [16], which allows the estimation of variable or unknown parameters of a system. The equation of the Luenberger observer is expressed in (5), where the symbol "^" denotes the estimated values:

$$\begin{cases} \dot{\hat{X}} = A(\omega_r)\hat{X} + BU + K\xi \\ \hat{Y} = C\hat{X} \end{cases} \quad (5)$$

where:

$\hat{X} = [\widehat{i_{s\alpha}}\ \widehat{i_{s\beta}}\ \widehat{\psi_{r\alpha}}\ \widehat{\psi_{r\beta}}]^T; \quad \hat{Y} = [\widehat{i_{s\alpha}}\ \widehat{i_{s\beta}}]^T;$

$\xi = [i_{s\alpha} - \widehat{i_{s\alpha}}\ \ i_{s\beta} - \widehat{i_{s\beta}}]^T$

Since there is no information about the measured currents, the vector ξ becomes:

$\xi = [-\widehat{i_{s\alpha}}\ \ -\widehat{i_{s\beta}}]^T$

The gain matrix K is defined as follows:

$$K = \begin{bmatrix} K_1 & K_2 & K_3 & K_4 \\ -K_2 & K_1 & -K_4 & K_3 \end{bmatrix}^T$$

where:

$$K_1 = (k-1)\left(\frac{1}{\sigma \tau_s} + \frac{1}{\sigma \tau_r}\right)$$

$$K_2 = -(k-1)\omega_r$$

$$K_3 = (k^2-1)\left[\left(\frac{1}{\sigma\tau_s}+\frac{1}{\sigma\tau_r}\right)\frac{\sigma L_s M}{L_r}-\frac{M}{\tau_r}\right] + \frac{\sigma L_s M}{L_r}\left(\frac{1}{\sigma\tau_s}+\frac{1}{\sigma\tau_r}\right)(k-1)$$

$$K_4 = -(k-1)\frac{\sigma L_s M}{L_r}\omega_r$$

with k a positive gain.

The estimation is performed throw the conservation of the state model (4) of the IM with the gain matrix K. This matrix ensures the convergence of the observer, and has been determined by the classical pole placement procedure. Then, replacing the adaptive mechanism by the measured rotational speed, as well as, feeding the observer with the stator voltages provided by the voltage synthesizer. This gives the stator currents estimation, as illustrated in Fig. 1.

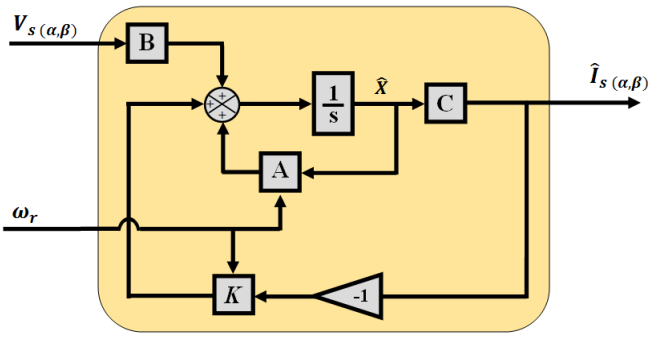

Fig. 1. Proposed stator currents estimator.

B. Fault Detection, Isolation and System Reconfiguration

The logic-circuit presented in Fig. 2 is intended to ensure the fault detection, isolation, and system reconfiguration. The detection of failures is performed by analyzing the residual signal between the measured and estimated quantities, passing through a Low Pass Filter (LFP) to extract the useful signal that will be compared to a well-defined threshold (Th=0.8), then a proper estimation is used for the isolation and reconfiguration of the system.

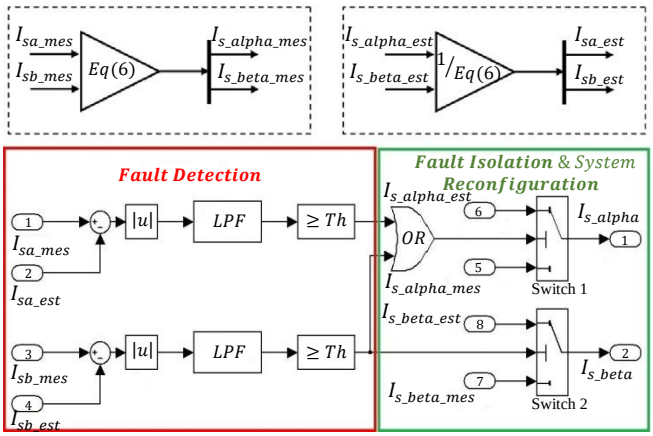

Fig. 2. Fault detection, isolation and system reconfiguration scheme

As mentioned previously, two current sensors (in phase-a and phase-b) were used in the proposed method for measuring a and b line currents. The axis transformation presented in Fig. 3 developed by [17] and used in both [18], and [19], which is also used in the proposed FTC, in order to have the component currents (α,β) using only the measurements of (a,b) components.

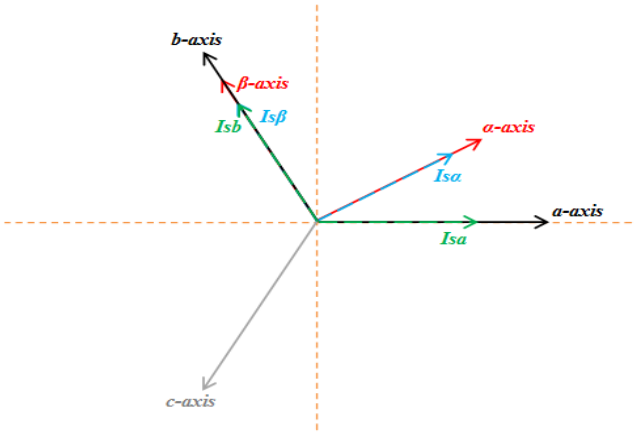

Fig. 3. Axis transformation model.

As shown in Fig. 3, the β-*axis* is aligned with the *b-axis*. Considering the equation of transformation from (a,b) to (α,β), which is given in (6), it is clear that $i_{s\alpha}$ depends on the two-phase currents I_{sa} and I_{sb}, whereas the current $i_{s\beta}$ depends only on the current I_{sb}. Therefore, if the phase-a current sensor becomes faulty, only $i_{s\alpha}$ that will be affected. But, if the phase-b current sensor becomes faulty, both currents $i_{s\alpha}$ and $i_{s\beta}$ will be affected.

$$\begin{bmatrix} i_{s\alpha} \\ i_{s\beta} \end{bmatrix} = \begin{bmatrix} 2/\sqrt{3} & 1/\sqrt{3} \\ 0 & 1 \end{bmatrix} \begin{bmatrix} I_{sa} \\ I_{sb} \end{bmatrix} \tag{6}$$

So, the faulty measured current components (α,β) must be replaced by the corresponding estimated currents. As a consequence, Table 1 shows the identification of the faulty sensors and the correct components of the estimated currents that will replace the erroneous components.

TABLE I. FAULTY SENSOR IDENTIFICATION AND CORRECT COMPONENT SELECTION

Sensor-a	Sensor-b	Za	Zb	OR	Proper selected components
Healthy	Healthy	**0**	**0**	**0**	$i_{s\alpha\ mes}$ and $i_{s\beta\ mes}$
Faulty	Healthy	**1**	**0**	**1**	$i_{s\alpha\ est}$ and $i_{s\beta\ mes}$
Healthy	Faulty	**0**	**1**	**1**	$i_{s\alpha\ est}$ and $i_{s\beta\ est}$
Faulty	Faulty	**1**	**1**	**1**	$i_{s\alpha\ est}$ and $i_{s\beta\ est}$

As presented in Fig. 2 and defined in Table I, it appears that in the case of *sensor-a* failure, fault detection part of the logic circuit generates an impulse Za=1, whereas, in the case of *sensor-b* failure, fault detection logic circuit generates an impulse Zb=1. Once the faulty sensor is identified, it is isolated, and the system is reconfigured, using the fault isolation and system reconfiguration part of the logic circuit. The logic gate OR output is 1 when any one of its inputs Za or Zb or both is 1 due to the effect of the failure of *sensor-b* on $i_{s\alpha}$ current. As a consequence, in the case of *sensor-b* failure, $i_{s\alpha\ mes}$ is isolated and replaced by $i_{s\alpha\ est}$.

IV. SIMULATION AND EXPERIMENTAL RESULTS

The proposed current sensor direct torque fault-tolerant control for induction motor drive is simulated in Matlab\Simulink environment using 4 kW induction motor parameters (see the Appendix). Fig. 4 presents the block diagram of the proposed method.

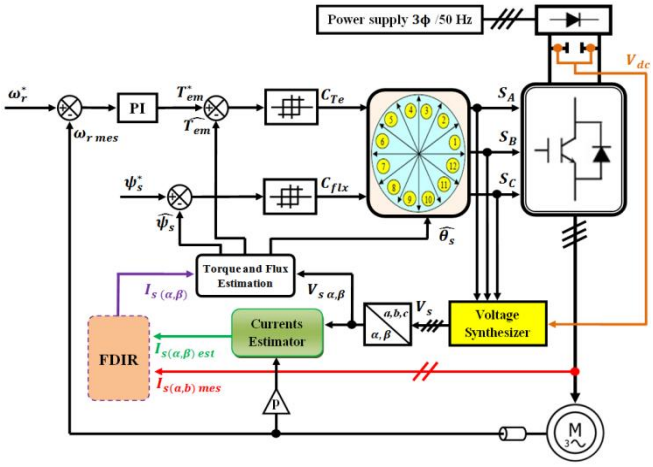

Fig. 4. Block diagram of the proposed FTC.

Fig. 5 displays the laboratory test bench in which the proposed control technique has been implemented and tested experimentally, which is composed mainly of a 4 kW three-phase IM whose parameters are the same used in simulation model, dS1104 card, two current sensors, and dc-voltage sensor.

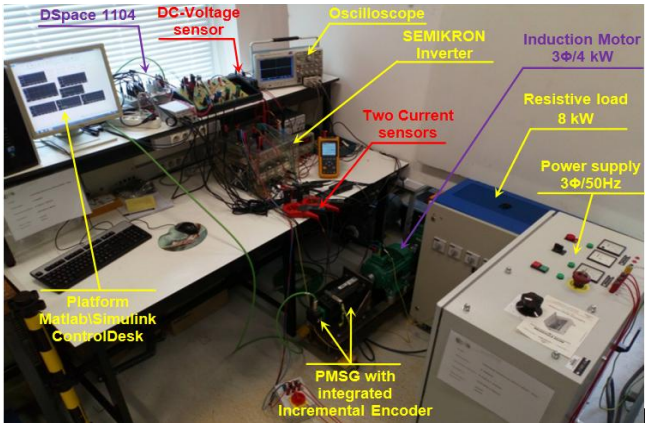

Fig. 5. Laboratory experimental test bench.

All simulation and experimental tests are performed at 1000 rpm with 20 N.m load torque.

A. *Test of the proposed FTC when sensor-a becomes faulty and sensor-b remains healthy*

Figs. 6 and 7 show simulation and experimental results obtained respectively, applying the proposed FTC. The drive was started with healthy current sensors in both simulation and experimentation. At t=1s in simulation test and t=10.6s in experimental test, current *sensor-a* fails. As a result and corresponding to the used axis transformation equation (6), $i_{s\alpha\ mes}$ becomes faulty such is depicted in Figs. 6(a) and 7(a), and $i_{s\beta\ mes}$ remains healthy as can be seen in Figs. 6(b) and 7(b). At the moment of failure occurrence, Za *sensor-a* state indicator becomes 1, judging *sensor-a* faulty, but Zb *sensor-b* state indicator remains 0, affirming that *sensor-b* is healthy, as illustrated in Figs. 6(c) and 7(c). As a consequence of Za=1, *switch-a* switches to input 1 to replace the erroneous measured current by the estimated one as explained previously in Table 1. Figs. 6(d), 7(d) and 6(e), 7(e) illustrate respectively the high-performance speed tracking of the IM drive, and the uninterrupted fulfillment of electromagnetic torque requirement under both healthy and faulty conditions, and Figs. 6(f), 7(f) depict stator flux circular trajectory.

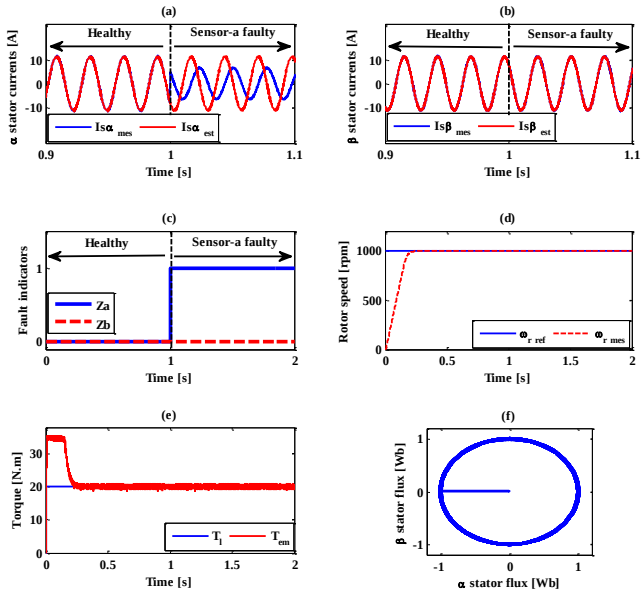

Fig. 6. Simulation results when *sensor-a* is faulty and *sensor-b* remains healthy: (a) $i_{s\alpha}$ currents, (b) $i_{s\beta}$ currents, (c) fault indicator, (d) reference and actual speeds, (e) load and electromagnetic torque, and (f) stator flux trajectory.

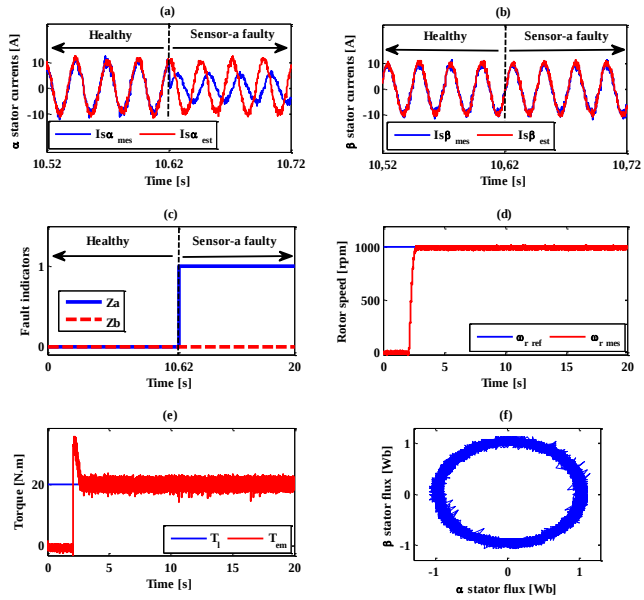

Fig. 7. Experimental results when *sensor-a* is faulty and *sensor-b* remains healthy: (a) $i_{s\alpha}$ currents, (b) $i_{s\beta}$ currents, (c) fault indicator, (d) reference and actual speeds, (e) load and electromagnetic torque, and (f) stator flux trajectory.

B. *Test of the proposed FTC when sensor-b becomes faulty and sensor-a remains healthy*

Figs. 8 and 9 give another test of the suggested FTC method with simulation and experimentation respectively, where a failure in *sensor-b* is performed, whereas *sensor-a* remains healthy. Simulation and experimental tests were started in healthy conditions until t=1s for simulation test and t=9.8s for experimental test, where *sensor-b* becomes faulty. Considering Figs. 8(a) and 9(a), it can be seen that $i_{s\alpha\ mes}$ is slightly affected by the failure of *sensor-b*, while $i_{s\beta\ mes}$ is significantly affected, which is explained previously in equation (6). The fault detection algorithm reacts quickly by generating an impulse Zb=1, indicating that *sensor-b* is faulty, unlike Za which remains at 0,

meaning that *sensor-a* gives proper measurement. At this moment, *switch-b* switches to input 1 to replace $i_{s\beta\ mes}$ by $i_{s\beta\ est}$, and according to the output of the gate OR (see Table 1) *switch-a* switches to input 1 to replace $i_{s\alpha\ mes}$ by $i_{s\alpha\ est}$. Figs. 8(c) and 9(c) demonstrate sensor state indicators Za and Zb. Figs. 8(d) for simulation and 9(d) for experimentation show the speed tracking performance of the IM drive before and after the failure occurrence.

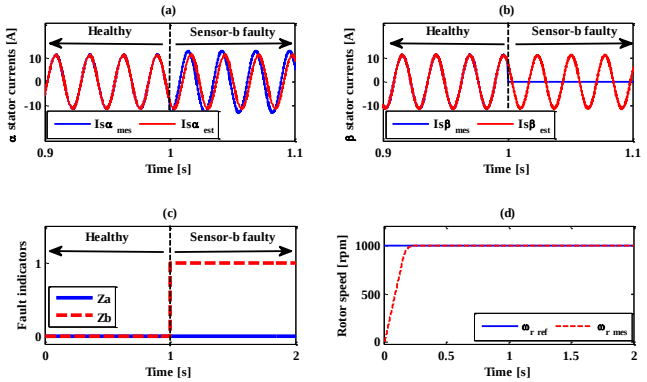

Fig. 8. Simulation results when *sensor-b* is faulty and *sensor-a* remains healthy: (a) $i_{s\alpha}$ currents, (b) $i_{s\beta}$ currents, (c) fault indicator, and (d) reference and actual speeds.

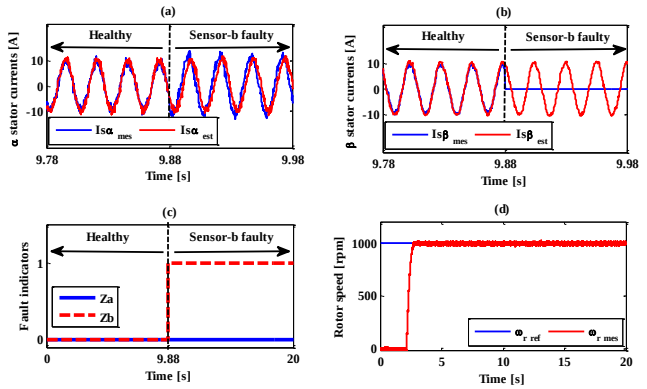

Fig. 9. Exprimental results when *sensor-b* is faulty and *sensor-a* remains healthy: (a) $i_{s\alpha}$ currents, (b) $i_{s\beta}$ currents, (c) fault indicator, and (d) reference and actual speeds.

C. Test of the proposed FTC when both sensor-a and sensor-b becom faulty

Figs. 10 and 11 illustrate respectively the simulation and experimentaion results obtained by applying the proposed FTC when the both sensors fail. The *sensor-a* failure is simulated at t=1s, while the *sensor-b* fault is simulated at t=1.1s as shown in the Figs. 10(a) and 10(b). In the experimental test, *sensor-a* failure is appeared at t=8.75s, while *sensor-b* failure is appeared at t=14.35s as can be seen in Figs. 11(a) and 11(b). While, Figs. 10(c) and 11(c) show the fault indicator signals (Za for *sensor-a* and Zb for *sensor-b*). When the defect is suddenly introduced in the *sensor-a*, the fault detection mechanism has reacted quickly by generating a Za index equal to 1, indicating that *sensor-a* is faulty. Based on equation (6), the current $i_{s\beta\ mes}$ will not be affected, which is visible in Figs. 10(b) and 11(b), where the current $i_{s\beta\ mes}$ remains healthy from 0 to 1.1s in simulation and until 14.34s in experimentation. According to Table 1, the selected currents to isolate the faulty measurement are: $i_{s\alpha\ est}$ and $i_{s\beta\ mes}$. After 1.1s in simulation and 14.35s in experimentation, a fault has been introduced in *sensor-b*, at this moment, the fault indicator Zb becomes 1, confirming *sensor-b* failure. Referring to equation (6), we can see that the currents $i_{s\alpha}$ and $i_{s\beta}$ both depend on the state of the measurment of *sensor-b*, which is confirmed in Figs. 10(a) and 11(a) where the degree of severity of the fault in the current $i_{s\alpha\ mes}$ is increased. Therefore, the isolation and reconfiguration algorithm chooses $i_{s\alpha\ est}$ and $i_{s\beta\ est}$ (see Table 1). Figs. 10(d), 11(d) and 10(e), 11(e) clearly show that speed and torque maintain their performance and remain uninterrupted, even under the worst possible conditions, when the both current sensors fail. In addition, Figs. 10(f) and 11(f) show the constant estimate of stator flux.

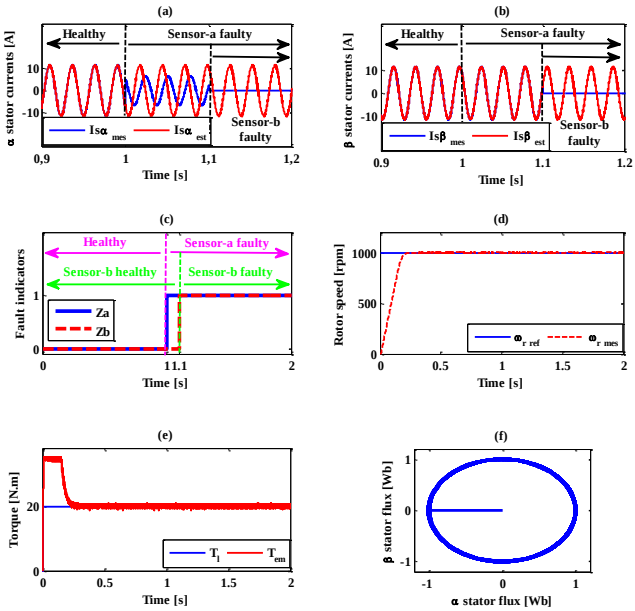

Fig. 10. Simulation results when both *sensor-a* and *sensor-b* becom faulty: (a) $i_{s\alpha}$ currents, (b) $i_{s\beta}$ currents, (c) fault indicator, (d) reference and actual speeds, (e) load and electromagnetic torque, and (f) stotor flux trajectory.

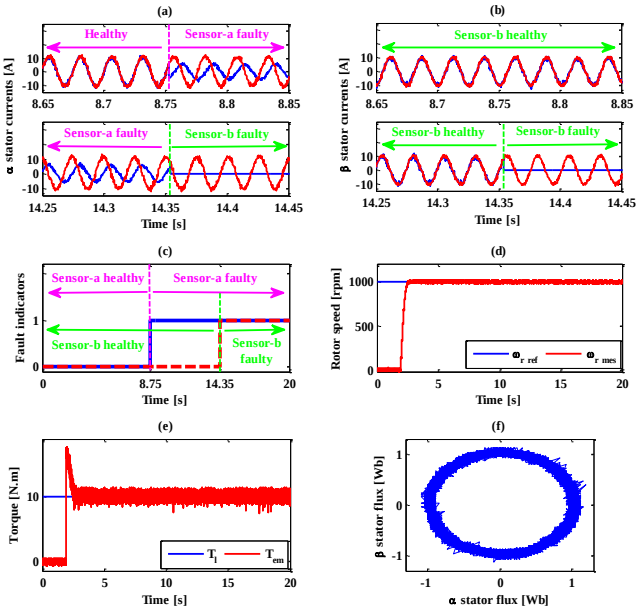

Fig. 11. Exprimental results when both *sensor-a* and sensor-b becom faulty: (a) $i_{s\alpha}$ currents, (b) $i_{s\beta}$ currents, (c) fault indicator, (d) reference and actual speeds, (e) load and electromagnetic torque, and (f) stotor flux trajectory.

V. Conclusion

This paper presents a direct torque fault-tolerant control diagram for current sensors failures in the induction motor drives. For the identification of a sensor failure, a logic circuit is used in the phases where the current sensors are located, which is able to detect the failures of the used current sensors. A current estimator is used to estimate the stator currents. Immediately after the failure of the current sensor, a decision logic circuit automatically selects the correct current signal to maintain the operation of the system. Simulation and experimental results show the effectiveness of the proposed method, where the fault detection is accomplished with fast dynamics, and the drive is performing successfully, without compromising the control system.

Appendix

Specifications		Parameters	
Nominal power [kW]	4	R_s [Ω]	1.5
Nominal voltage [V]	400	R_r [Ω]	2.03
Nominal current [A]	9.2	L_s [H]	0.36
Frequency [Hz]	50	L_r [H]	0.36
Number of pole pairs	2	M [H]	0.35
Nominal speed [rpm]	1415	J [Kg.m^2]	0.024
		f [Nm.s.rad^{-1}]	0.002

Acknowledgment

This work has been achieved within the framework of CE2I project (Convertisseur d'Energie Intégré Intelligent). CE2I is co-financed by European Union with the financial support of the European Regional Development Fund (ERDF), French State and the French Region of Hauts-de-France.

As well, this work was supported by the European Regional Development Fund (ERDF) through the Operational Program for Competitiveness and Internationalization – COMPETE 2020, and also by National Funds through the Portuguese Foundation for Science and Technology (FCT), under Project POCI-01-0145-FEDER-029494 and Project UID/EEA/04131/2013.

References

[1] H. Berriri, M. W. Naouar, and I. Slama-Belkhodja, "Easy and Fast Sensor Fault Detection and Isolation Algorithm for Electrical Drives," *IEEE Trans. Power Electron.*, vol. 27, no. 2, pp. 490–499, Feb. 2012.

[2] Y. Yu, X. Chen, and Z. Dong, "Current sensorless direct predictive control for induction motor drives," in *2017 IEEE Transportation Electrification Conference and Expo, Asia-Pacific (ITEC Asia-Pacific)*, 2017, no. August, pp. 1–6.

[3] C. Gajanayake, B. S. Bhangu, G. Foo, X. Zhang, K. J. Tseng, and M. Don Vilathgamuwa, "Sensor fault detection, isolation and system reconfiguration based on extended Kalman filter for induction motor drives," *IET Electr. Power Appl.*, vol. 7, no. 7, pp. 607–617, Aug. 2013.

[4] M. Dybkowski and K. Klimkowski, "Stator current sensor fault detection and isolation for vector controlled induction motor drive," in *2016 IEEE International Power Electronics and Motion Control Conference (PEMC)*, 2016, pp. 1097–1102.

[5] K.-S. Lee and J.-S. Ryu, "Instrument fault detection and compensation scheme for direct torque controlled induction motor drives," *IEE Proc. - Control Theory Appl.*, vol. 150, no. 4, pp. 376–382, Jul. 2003.

[6] T. A. Najafabadi, F. R. Salmasi, and P. Jabehdar-Maralani, "Detection and Isolation of Speed-, DC-Link Voltage-, and Current-Sensor Faults Based on an Adaptive Observer in Induction-Motor Drives," *IEEE Trans. Ind. Electron.*, vol. 58, no. 5, pp. 1662–1672, May 2011.

[7] Y. Yu, Z. Wang, D. Xu, T. Zhou, and R. Xu, "Speed and Current Sensor Fault Detection and Isolation Based on Adaptive Observers for IM Drives," *J. Power Electron.*, vol. 14, no. 5, pp. 967–979, Sep. 2014.

[8] Y. Yu, Y. Zhao, B. Wang, X. Huang, and D. Xu, "Current Sensor Fault Diagnosis and Tolerant Control for VSI-Based Induction Motor Drives," *IEEE Trans. Power Electron.*, vol. 33, no. 5, pp. 4238–4248, May 2018.

[9] A. M. S. Mendes and A. J. Marques Cardoso, "Fault-Tolerant Operating Strategies Applied to Three-Phase Induction-Motor Drives," *IEEE Trans. Ind. Electron.*, vol. 53, no. 6, pp. 1807–1817, Dec. 2006.

[10] Y. Azzoug, A. Menacer, R. Pusca, R. R. Romary, T. Ameid, and A. Amma, "Fault Tolerant Control for Speed Sensor Failure in Induction Motor Drive based on Direct Torque Control and Adaptive Stator Flux Observer," in *2018 International Conference on Applied and Theoretical Electricity (ICATE)*, 2018, pp. 1–6.

[11] M. Stettenbenz, Y. Liu, and A. Bazzi, "Smooth switching controllers for reliable induction motor drive operation after sensor failures," in *2015 IEEE Applied Power Electronics Conference and Exposition (APEC)*, 2015, pp. 2407–2411.

[12] Y. Liu, M. Stettenbenz, and A. M. Bazzi, "Smooth Fault-Tolerant Control of Induction Motor Drives with Sensor Failures," *IEEE Trans. Power Electron.*, vol. PP, no. c, pp. 1–1, 2018.

[13] R. B. Sepe, B. Fahimi, C. Morrison, and J. M. Miller, "Fault tolerant operation of induction motor drives with automatic controller reconfiguration," in *IEMDC 2001. IEEE International Electric Machines and Drives Conference (Cat. No.01EX485)*, pp. 156–162.

[14] F. Aguilera, P. M. de la Barrera, and C. H. De Angelo, "A fault tolerant system for current sensors in induction motor drives," in *2015 XVI Workshop on Information Processing and Control (RPIC)*, 2015, pp. 1–7.

[15] B. Tabbache, N. Rizoug, M. E. H. Benbouzid, and A. Kheloui, "A Control Reconfiguration Strategy for Post-Sensor FTC in Induction Motor-Based EVs," *IEEE Trans. Veh. Technol.*, vol. 62, no. 3, pp. 965–971, Mar. 2013.

[16] D. Luenberger, "An introduction to observers," *IEEE Trans. Automat. Contr.*, vol. 16, no. 6, pp. 596–602, Dec. 1971.

[17] C. Chakraborty and V. Verma, "Speed and Current Sensor Fault Detection and Isolation Technique for Induction Motor Drive Using Axes Transformation," *IEEE Trans. Ind. Electron.*, vol. 62, no. 3, pp. 1943–1954, Mar. 2015.

[18] M. Manohar, S. Das, and R. Kumar, "A robust current sensor fault detection scheme for sensorless induction motor drive," in *2017 IEEE PES Asia-Pacific Power and Energy Engineering Conference (APPEEC)*, 2017, pp. 1–6.

[19] M. Manohar and S. Das, "Current Sensor Fault-Tolerant Control for Direct Torque Control of Induction Motor Drive Using Flux-Linkage Observer," *IEEE Trans. Ind. Informatics*, vol. 13, no. 6, pp. 2824–2833, Dec. 2017.